International Journal of Mechanical, Industrial and Aerospace Sciences
ISSN: 2517-9950
Vol:10, No:2, 2016

Numerical Analysis of the Turbulent Flow around DTMB 4119 Marine Propeller

K. Boumediene, S. E. Belhenniche

***Abstract*—**This article presents a numerical analysis of a turbulent flow past DTMB 4119 marine propeller by the means of RANS approach; the propeller designed at David Taylor Model Basin in USA. The purpose of this study is to predict the hydrodynamic performance of the marine propeller, it aims also to compare the results obtained with the experiment carried out in open water tests; a periodical computational domain was created to reduce the unstructured mesh size generated. The standard kw turbulence model for the simulation is selected; the results were in a good agreement. Therefore, the errors were estimated respectively to 1.3% and 5.9% for KT and KQ.

***Keywords*—**Propeller flow, CFD simulation, hydrodynamic performance, RANS.

I. Introduction

DUE to the geometric form of the ship's stern region; the velocity field is considered as non-uniform close to the propeller [6]. Numerical methods were used to predict the flow in the said region such as RANS and LES methods using commercial software or open source programs. Fast evolution of computer technologies and set of numerical calculation methods which are becoming more and more precise, has led to the obtainment of significant results.

The computational fluid dynamics was used as analytical and experiment methods and has proved its efficiency for validation of benchmark data.

The marine propeller is a complex geometry; with profiles for different sections, chords lengths, and geometric pitch angles of variable pitch [2]. The RANS method has proved its reliability to predict the viscous flow around marine propeller. The quality of the mesh and turbulence modeling are the main obstacles influential on the accuracy of results. [2]

In order to check the reliability of the numerical simulation; the results were compared with experimental outcomes achieved from the open water tests.

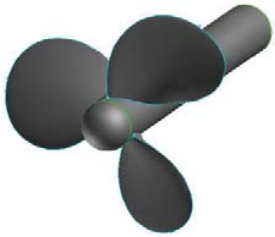

Fig. 1 Main Particulars of the Propeller

Kadda Boumediene is with the University of Sciences and Technology of Oran, Algeria (e-mail: kadda.boumediene@univ-usto.dz).

TABLE I
Notations and Symbols

Symbol	Definition	Unit
J	Advance coefficient	-
K_T	Thrust coefficient	-
K_Q	Torque coefficient	-
Va	Propeller advance velocity	m/s
Re	Reynolds number	-
Cp	Propeller pressure coefficient	-
n	Propeller pressure coefficient	rps
D	Propeller revolution	m
P	Propeller Pitch	m
η_0	Propeller efficiency in open water	-
η_B	Propeller efficiency behind a hull	-

II. Geometric Characteristics of DTMB 4119 Propeller

The DTMB 4119 marine propeller model was designed at United States (David Taylor Model Basin), it is a three blades submerged non-cavitating propeller, with a variable pitch and a diameter of D = 0.3048 m. The geometric characteristics of the marine propeller are illustrated in Tables II, III.

TABLE II
Main Particulars of the Propeller

DTMB 4119	
Number of Blade [-]	3
Propeller diameter[m]	0.3048
Pitch [-]	Variable
Material	Ni-Al-Bz

TABLE III
Geometry of Original DTMB 4119 Propeller

r/R	c/D	P/D	T/c	F/c
0.2	0.3200	1.1050	0.20550	0.01429
0.3	0.3625	1.1020	0.15530	0.02318
0.4	0.4048	1.0980	0.11800	0.02303
0.5	0.4392	1.0930	0.09160	0.02182
0.6	0.4610	1.0880	0.06960	0.02072
0.7	0.4622	1.0840	0.05418	0.02003
0.8	0.4347	1.0810	0.04206	0.01967
0.9	0.3613	1.0790	0.03321	0.01817
0.95	0.2775	1.0770	0.03228	0.01631
1	0.0000	1.0750	0.03160	0.01175

III. Mathematical Formulation

The turbulent viscous flow around the propeller is described by the Navier-Stokes and turbulent equations as:

$$\frac{\partial u_i}{\partial x_i} = 0 \quad (1)$$

$$\frac{\partial(\rho u_i)}{\partial t} + \frac{\partial(\rho u_i u_j)}{\partial x_j} = -\frac{\partial P}{\partial x} + \frac{\partial}{\partial x_j}\left(\mu \frac{\partial u_i}{\partial x_j} - \overline{\rho u_i' u_j'}\right) \quad (2)$$

A. The Standard $k-\omega$ Turbulence Model

The Wilcox [1] *k-ω* two-equation model is given by the following turbulent kinetic energy and dissipation equations:

$$\frac{\partial(\rho k)}{\partial t} + \frac{\partial(\rho u_j k)}{\partial x_j} = P - \beta^* \rho \omega k + \frac{\partial}{\partial x_j}\left[\left(\mu + \sigma_k \frac{\rho k}{\omega}\right)\frac{\partial k}{\partial x_j}\right] \quad (3)$$

$$\frac{\partial(\rho \omega)}{\partial t} + \frac{\partial(\rho u_j \omega)}{\partial x_j} = \frac{\gamma \omega}{k} P - \beta \rho \omega^2 + \frac{\partial}{\partial x_j}\left[\left(\mu + \sigma_\omega \frac{\rho k}{\omega}\right)\frac{\partial \omega}{\partial x_j}\right] + \frac{\rho \sigma_d}{\omega}\frac{\partial k}{\partial x_j}\frac{\partial \omega}{\partial x_j} \quad (4)$$

Explicit details for the model can be found in [9] and [10].

IV. Numerical Procedure

The commercial code Fluent 6.3.26 [7] based on the finite volume method was used for the simulation. To close the system of equations we select the standard kw model. Simple solver for coupling pressure-velocity, and we selected QUICK scheme for the discretization of the terms of diffusion and convection.

For discretization of the momentum equation, we adopt The STANDARD scheme and we chose the first order of UPWIND scheme for energy and dissipation.

V. Mesh and Boundary Conditions

To minimize the number of elements and time of simulation; a periodic domain was performed on Gambit [4], [8], the computational was divided into 6 blocks to control the mesh with a small block surrounding the blade. Fig. 2 shows the computational domain done in Gambit.

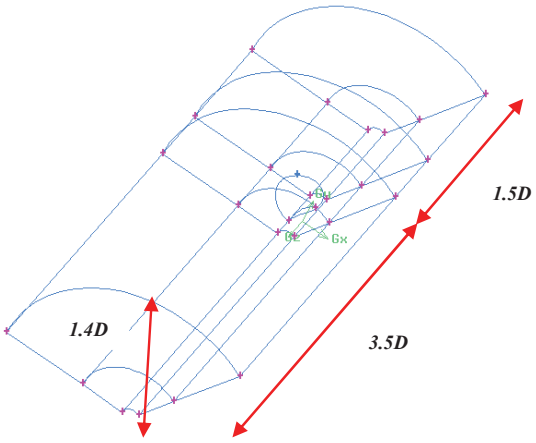

Fig. 2 Computational Domain

We adopt a hybrid mesh, we mesh the first blade with constant tetrahedral cells with a size of 0.005D as illustrated in Fig. 3, and however we mesh other blocks with hexahedral cells as shown in Fig. 4.

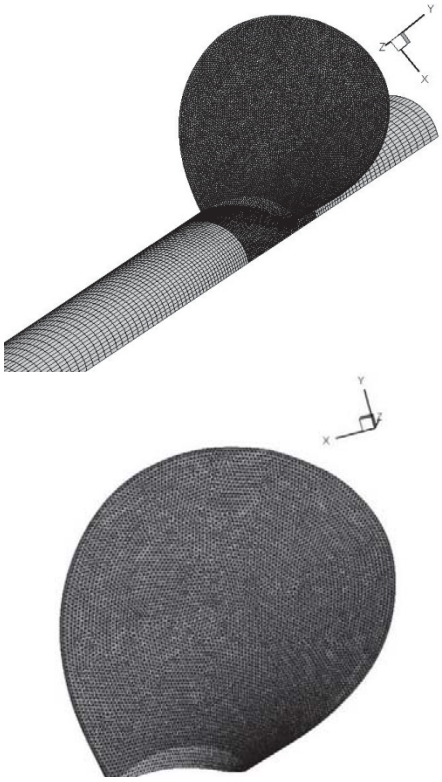

Fig. 3 Mesh for blade and shaft line

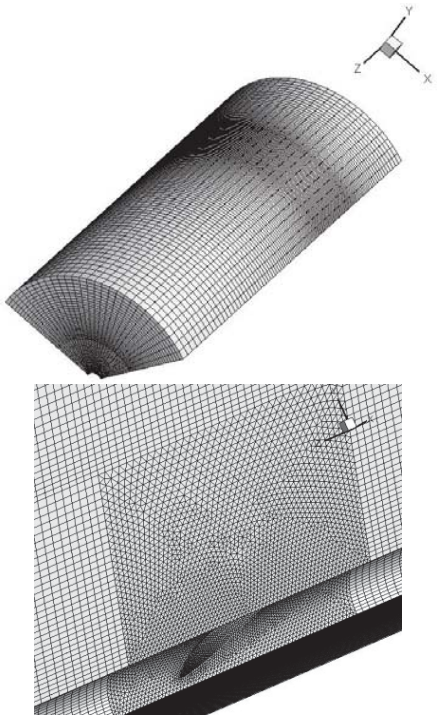

Fig. 4 The grid of the domain

Table III shows the mesh method used for the 6 blocks; A local grid mesh was adopted i.e. constant and exponential on

the edges of the 6 blocks to control a grid. The inlet is located at 1.5D characterized by a uniform velocity which depends on the advance coefficient J [4], a static pressure is located at the at 3.5D, and the slip condition on the outer boundary of the computational domain; however, the non-slip condition is applied for the shaft and the 3 blades. The fluid is considered rotational around the z axis using Moving Reference Frame (MRF).

VI. Initial Conditions

Steady numerical simulating was achieved for a wide range of advance coefficients J between 0.5 and 1.1.

The rotational speed of the propeller model DTMB 4119 was fixed at n = 10 rps.

TABLE IV
INITIAL CONDITIONS

DTMB 4119	
n [rps]	10
V_a [m/s]	2.54
J[-]	0.833
K_T[-]	0.15

VII. Open Water Results

The numerical results are compared with experiment for a wide range of advance coefficients J. Fig. 5 shows the calculated hydrodynamic performance KT and 10KQ compared with experiment results; the red lines are the numerical results and the green lines are those of the experimental. The obtained results are in good agreement with the experiment results [3] and the mean error estimated for the thrust coefficient KT is 1.3% and 5.9 % for torque coefficient KQ.

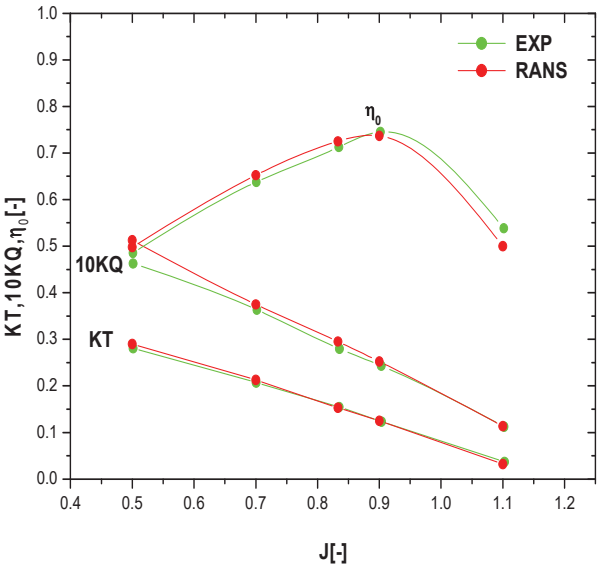

Fig. 5 Open water characteristics of DTMB 4119 propeller

TABLE V
NUMERICAL AND EXPERIMENTAL RESULTS

J	K_T EXP	K_T RANS	$10K_Q$EXP	$10K_Q$ RANS
0.5	*0.281*	*0.29*	*0.463*	*0.512*
0.7	*0.207*	*0.213*	*0.363*	*0.375*
0.833	*0.155*	*0.153*	*0.280*	*0.295*
0.9	*0.123*	*0.125*	*0.243*	*0.252*
1.1	*0.037*	*0.032*	*0.112*	*0.113*

Fig. 6 shows the pressure coefficient contour *Cp* for different advance coefficient J. It is clearly shown that the pressure coefficient is constant over for the blades since the flow is uniform at the inlet; however, it changes if the propeller is operating behind the ship hull [5].

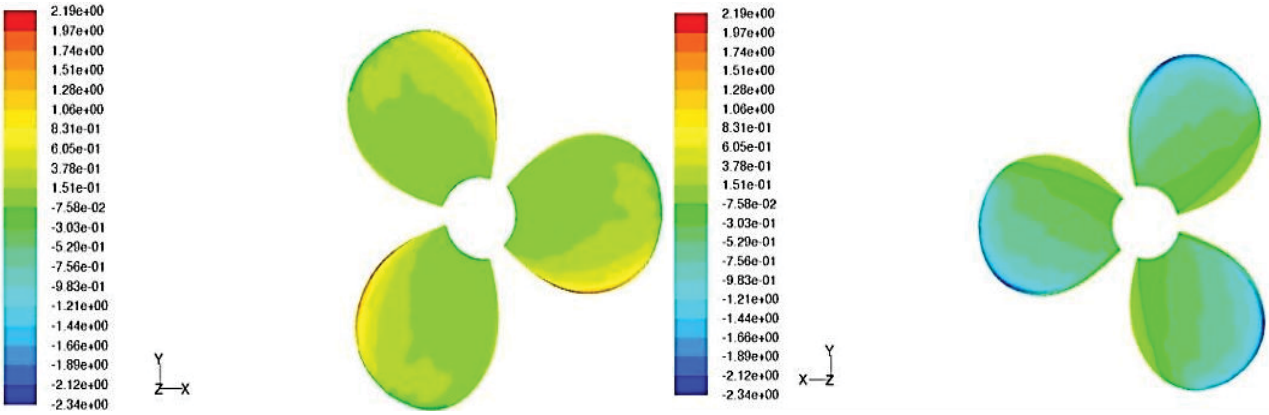

(a) J=0.5

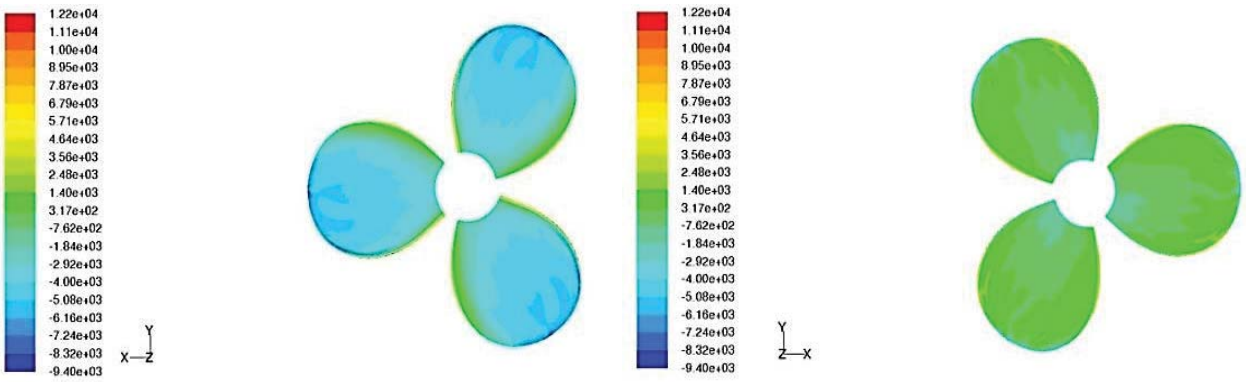

(b) *J=0.833*

Fig. 6 Pressure distribution on the blade suction and pressure sides

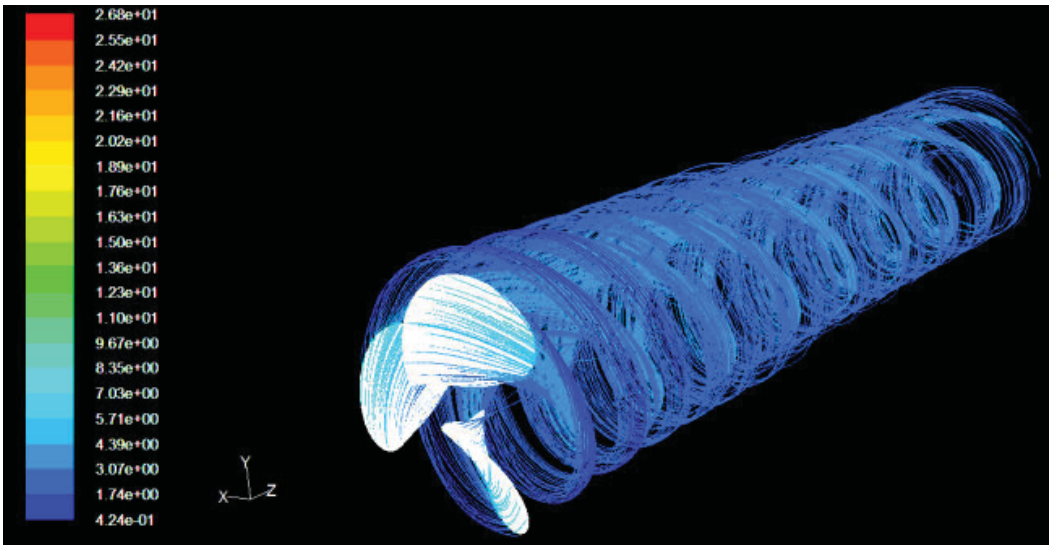

(a) *J=0.5*

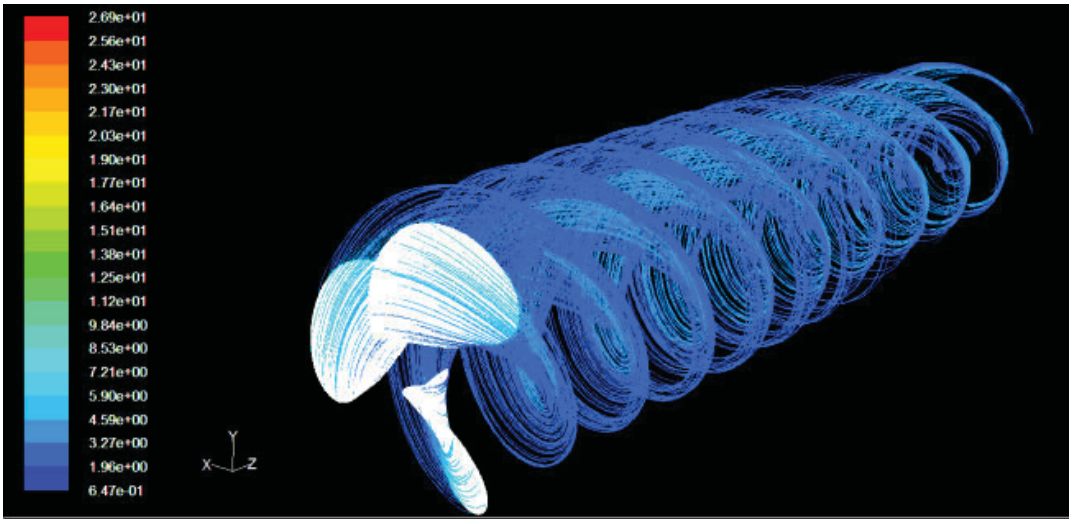

(b) J=0.833

Fig. 7 The streamlines for different advance coefficients J

The pressure coefficient CP at 0.3R for advance coefficient J = 0.833 is illustrated on the Fig. 8. The numerical results are presented by redpoints, however the experiment one are with green points. The obtained values agree well with the experiment results.

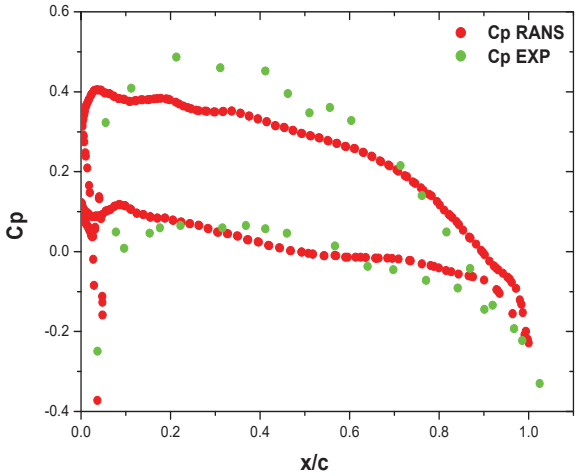

Fig. 8 Pressure Coefficient Contour *Cp*

VIII. Conclusion

A numerical simulation of a turbulent flow around DTMB 4119 marine propeller was carried out to predict the open water characteristics and compare the results with the experiment a periodic domain with an unstructured mesh was used.

The simulation was performed for a uniform steady flow depending on the advance coefficient J between 0.5 and 1.1 [4]. The CFD results were compared with the experiment outcomes; the difference is less than 1.3% for K_T and 5.9% for K_Q.

References

[1] Wilcox, D.C., Turbulence Modeling for CFD, 2nd Ed., DCW Industries, Inc., La Canada, CA, 1998.
[2] Marine propeller and propulsion John Carlton, 2ndEdition Great Britain, MPG Books Ltd, Bodmin Cornwall, 2007.
[3] Jessup. S.D., "An experimental investigation of Viscous Aspects of Propeller Blade Flow Experiments" The Catholic University of America.
[4] L.d. Qing "Validation of RANS Predictions of Open Water Performance of a Highly Skewed Propeller with Experiments" Conference of Global Chinese Scholars on Hydrodynamics
[5] S.E. Belhenniche "Application of CFD in Analysis of Steady and Unsteady Turbulent Flow Past a Marine Propeller "International Conference of Heat and Mass Transfer ICHMT Palermo (Italy) 2012.
[6] Architecture Navale Dominique Presles, Edition de la Villette, Paris 2005.
[7] Ansys Fluent 6.3.26
[8] Gambit 2.3.16
[9] Wilcox, D.C., 2006, Turbulence Modeling for CFD, 3rd Ed., DCW, Industries, Inc., La Canada, CA.
[10] Menter, F., 1994.Two-equationeddy- viscosity turbulence model for engineering applications, AIAAJ., 32(8):1598-1605